



# Copper, brass and bronze strips with controlled properties by RCS method

**W. Głuchowski<sup>a,\*</sup>, J. Domagała-Dubiel<sup>a</sup>, J. Sobota<sup>a</sup>,  
J. Stobrawa<sup>a</sup>, Z. Rdzawski<sup>a,b</sup>**

<sup>a</sup> Institute of Non-Ferrous Metals, ul. Sowińskiego 5, 44-100 Gliwice, Poland

<sup>b</sup> Institute of Engineering Materials and Biomaterials, Faculty of Mechanical Engineering,  
Silesian University of Technology, ul. Konarskiego 18a, 44-100 Gliwice, Poland

\* Corresponding e-mail address: wojciech.gluchowski@imn.gliwice.pl

Received 21.02.2013; published in revised form 01.04.2013

## ABSTRACT

**Purpose:** A growing trend to use the copper-based strips is observed recently world-wide in the electric and electronic industry. Ultrafine grained copper and solid solution hardened copper alloys are applied where high electrical conductivity and good mechanical properties are required.

**Design/methodology/approach:** This study was aimed to investigate microstructure in strips of copper alloys with different stacking fault energy value. The investigated materials have been processed by one of the severe plastic deformation method, using different variants of continuous repetitive corrugation and straightening (CRCS). Deformation was executed by parallel and perpendicular corrugation and straightening of strip sample.

**Findings:** Continuous repetitive corrugation and straightening is a promising method for refining of microstructure of metallic strips.

**Practical implications:** A growing trend to use copper brass and bronze strips with improved functional properties is observed recently world-wide. Within this group of materials particular attention is drawn to those with ultra fine or nanometric grain size.

**Originality/value:** The paper contributes to the microstructure evolution of solid solution hardened and age-hardened copper alloys strips produced by original RCS method.

**Keywords:** Metallic alloys; Severe Plastic Deformation; Mechanical properties; Refined microstructure

**Reference to this paper should be given in the following way:**

W. Głuchowski, J. Domagała-Dubiel, J. Sobota, J. Stobrawa, Z. Rdzawski, Copper, brass and bronze strips with controlled properties by RCS method, Archives of Materials Science and Engineering 60/2 (2013) 53-63.

## MATERIALS

### 1. Introduction

Severe Plastic Deformation (SPD) has been widely used to refine the grain structure of metals and alloys. The most popular SPD methods include Equal Channel Angular Pressing (ECAP), Hydrostatic Extrusion (HE), High-Pressure Torsion (HPT), Cyclic

Extrusion-Compression (CEC), Multiaxial Forging (MF), Accumulative Roll-Bonding (ARB), GP techniques, Max-Strain cumulative plastic deformation, Repetitive Corrugation and Straightening (RCS) [1-5].

Grain refinement produced by SPD method ranges from 1  $\mu\text{m}$  to about 100 nm, while subgrains, dislocation cells and crystallites present much smaller dimension, below 100 nm. Dislocation

model for determination of minimum grain size in severe deformations during milling process was presented by Mohamed [6]. One of the fundamental assumptions of that model is Fecht's phenomenological approach [7] according to which the grain refinement consists of three stages: (a) location of dislocations of high density in shearing bands; (b) annihilation and recombination of dislocations which leads to formation of cells and subgrains (recovery), and (c) transformation of subgrain boundaries into high-angle boundaries. That line of reasoning suggests that the minimum grain size  $d_{\min}$  in that process results from the balance between dislocation structure, as introduced by intensive deformation, and its thermal recovery. According to that model the  $d_{\min}$  depends on the applied stress, value of stacking fault energy and activation energy of recovery process. When stress and activation energy are constant the  $d_{\min}$  value changes with the standard value of stacking fault energy according to the formula (1):

$$\frac{d_{\min}}{b} = A \left( \frac{\gamma}{Gb} \right)^q \quad (1)$$

where: A is dimensionless constant, b is Burgers vector of dislocation,  $\gamma$  is stacking fault energy, G is rigidity modulus and  $q=0.5$  is exponent of standard stacking fault energy.

The stacking fault energy, which determines the width of stacking fault band between two Shockley partial dislocations, controls the rate of cross slip and climb of dislocation. With the decrease of that energy also role of deformation by twinning in the general deformation mechanism and, in consequence, in mechanism of microstructure refinement should be increasing.

The Mohamed model is based on the data obtained in microstructure refinement processes in high-energy planetary mills but it can be also used in analysis of microstructure refinement mechanism in other processes. A similar microstructure refinement mechanism in copper during application of large plastic deformation was observed by Mishra et al [8]. The authors also demonstrated large influence of adiabatic shearing bands in this process [8,9].

Microstructure refinement brings improvement of mechanical properties of metals according to the Hall-Petch relation, where the yield stress value is a function of the inverse of the square root of mean grain diameter. In submicron and nanocrystalline materials that dependency collapses. The reduction of yield point is explained by the change of deformation mechanism which starts to prevail when grain size exceeds a critical value.

The RCS process provides possibility to produce a microstructure refinement effect in microstructure of strips. The repetitive corrugation and straightening can also be performed by application of pressing between grooved plates or rolling with toothed and flat rolls. Because of the continuity of the process its main advantage is a possibility for production of significant volumes of the material in a strip form and relatively simple upscaling from laboratory to pilot and even industrial conditions [10-18]. Application of materials of nano- or submicron structure, however, requires broadening of the knowledge on their functional properties.

The objective of this study was to determine influence of repetitive corrugation and straightening (RCS) on microstructure

and properties of copper and its alloys (CuZn36, CuSn6) when compared to the strips in the initial (annealed) state and also after RCS process and next annealed. Those alloys, in comparison to copper, present significantly lower stacking fault energy.

## 2. Material and methodology

Samples of strips made of Cu, CuZn36 of dimensions 140x25x1 mm and CuSn6 of dimensions 140x25x0.8 mm were annealed for 1 hour in temperature of 550°C in electric resistance furnace. Thus prepared samples were subjected to repetitive corrugation and straightening. The complete cycle included: bending on toothed rolls, straightening on flat rolls, bending on grooved rolls, straightening on flat rolls (four passes in total). The sample was turned around by 180° after each cycle. To determine the maximum number of cycles N max (critical actual deformation) the cycles were repeated until the sample got broken. The strips were also deformed in 1/3 and 2/3 of the critical number of cycles (Table 1); for copper it was 42 and 21 cycles, for brass 36 and 18 cycles, while for bronze it was 52 and 26 cycles, respectively. In thus conducted tests deformation in a single cycle was 0.58 [19]. Samples of strips after RCS process were annealed for 1 hour in temperature of 550°C.

Table 1.

Number of full cycles and value of deformation for different grades of strips subjected to repetitive corrugation and straightening

	maximum	2/3	1/3
Cu	63	42	21
	36.5	24.4	12.2
CuZn36	59	36	18
	34.2	20.9	10.4
CuSn6	78	52	26
	45.2	30.2	15.1

Microstructure of examined materials was investigated with metallographic microscopy. Grain size, crystallographic orientation of grains in the strips after 1 hour annealing in temperature of 550°C, deformed in repetitive corrugation and straightening and deformed by RCS process and next annealed was determined by scanning microscope equipped with Electron Backscatter Diffraction (EBSD) detector.

TEM investigation were performed using electron microscope.

Hardness was measured by Vickers method. Tension test were performed with flat samples in INSTRON testing machine. Electrical conductivity was measured by eddy-current Foerster Sigmatest.

The industrial test was carried out on CuSn6 strip (in the cold deformed state) 0.64 x184 mm in cross-section. The strip was passed through straighten-stretcher with a modified system of corrugation and straightening rolls. For this material the microstructure, mechanical properties and hardness research have been conducted.

### 3. Results and discussion

#### 3.1. Laboratory tests

To determine influence of microstructure refinement degree on hardening mechanism in copper and its alloys (CuZn36, CuSn6) in RCS process the materials in the initial state (annealed for 1 hour in temperature of 550°C), after deformation by RCS process and the next annealed for 1 hour in temperature of 550°C were examined. Microstructure of copper after recrystallization annealing shows visible annealing twins, resulting from the middle stacking fault energy of that metal (Fig. 1). CuZn36 alloys are characterized by single-phase structure of the basic solution  $\alpha$ , of polyhedral grains with numerous annealing twins (Fig. 4), while microstructure of CuSn6 strips with visible crystals of alpha phase with twins is shown in Fig. 7.

After repetitive corrugation and straightening the analyzed structures of CuSn6 strip deformation show clearly marked slip systems (Fig. 8). They are limited to the area of grain interior and only occasionally show tendency for going beyond grain boundaries. Also shearing bands become visible along the directions of maximal non-dilational (shearing) strains.

Microstructure of Cu, CuZn36, CuSn6 strips after RCS process and the next annealing is similar to microstructure in the initial state (Figs. 3, 6, 9).

Test results using the EBSD detector (backscattered electron diffraction) are shown in Figs. 1-9 c. Based on data obtained using EBSD detector was obtained including crystallographic information on material. The use of EBSD technique was to investigate the effect of the cyclical process of corrugation and straightening of the fraction of development of grain boundaries, both narrow-and wide-angle, and thus the level of fragmentation of the structure. The strips of copper and its alloys after cyclic corrugation and straightening prevail grain boundaries narrow angle involving a range of 2-15° (72-78%), while in the initial material in a wide angle range 15-180°. For the material deformed by the RCS process, and then annealed at 550°C/1h fraction of development of narrow angle for Cu is 42.8%, whereas for copper alloys CuZn36 and CuSn6 - 4.8% and 8.2%, respectively.

Texture samples of Cu, CuZn36 and CuSn6 strips (Fig. 10) in the initial state is similar and can be described as very weak texture mill, which dominate grain orientation near  $\{112\} \langle 111 \rangle$  and  $\{110\} \langle 112 \rangle$ . Jagged shape of the baseline in these figures indicates a coarsely crystalline nature of the material. Texture samples after repetitive corrugation and straightening is very similar in all the samples, regardless of the composition of the alloy. It differs significantly from the samples while after cold rolling. All samples after repetitive corrugation and straightening have texture in which the dominant component of the featured plane  $\{110\}$ . The system in pole Fig. maximum (four maximum near the middle of the projection, rotated relative to the rolling direction of about 45°) indicates that the texture is a double  $\{110\} \langle 112 \rangle$   $\{110\} \langle 111 \rangle$ , which partially overlap maxima at each other - or, texture  $\{110\} \langle 223 \rangle$  fuzzy by rotation around the axis  $\langle 110 \rangle$ . This can be seen especially broadening on the pole Figure of the sample strip CuSn6. Texture of the other samples

after repetitive corrugation and straightening exhibits significant asymmetry, which may be due to corrugation conditions, but may also be the result of the analysis of a limited number of crystallites. Texture analysis results show that during the process there is still a strong corrugation of the plastic deformation of the metal, resulting in the rotation of the crystal lattice of the grains as described above the position and thereby affecting the change of anisotropy of the properties of metal repetitive corrugation and straightening.

The average Cu grain size after RCS process is 9  $\mu\text{m}$ , CuZn36 - 8  $\mu\text{m}$ , while in CuSn6 it was 7  $\mu\text{m}$ . These values confirm that the average grain size decreases with reduction of stacking fault energy (SFE CuZn 35  $\text{mJ/m}^2$  [10] is significantly lower than Cu 78  $\text{mJ/m}^2$ , SFE CuSn - about 20  $\text{mJ/m}^2$  [20]). Lower SFE of the alloy facilitates grain refinement and the measured grain size is smaller, however the grain size reached by EBSD and TEM methods are different. To obtain unambiguous explanation of the mechanism of microstructure refinement and strain mechanism in ultra-fine and nanocrystalline materials it is necessary to precisely determine the size of grains/subgrains. Recently widely applied EBSD technique does not provide satisfactory results. The grain size measurements are disrupted by presence of texture, ultra-fine and nanocrystalline grains/subgrains, and also by resolving powers of determination of the lower limit of misorientation angle, therefore the measurements should be supplemented with laborious TEM measurements.

The grain/subgrain size in strips made of Cu and its alloys after RCS process is in the range 50-300 nm (Figs. 2d, 4d, 6d). Also areas with shearing bands can be observed. In majority of grains/subgrains presence of large dislocation density was established.

Beside typical grain structure, produced in the result of crossing of numerous deformation bands, the refined material presents structure composed of dislocation cells and subgrains.

Both tensile strength and 0.2 yield strength of Cu, CuZn36 and CuSn6 strips after deformation by repetitive corrugation and straightening increase when compared to strips after annealing, while after deformation by RCS process and the next annealing are comparable to the values obtained for the material in the initial state. (Figs. 11, 12).

Elongation  $A_{50}$  of strip samples after deformation by repetitive corrugation and straightening significantly drops when compared to the samples in the initial state, from 43% to about 4.5% for copper, from 48% to about 6.5% for strip sample of CuZn36 and from 41% to about 7% for CuSn6 (Fig. 13).

Hardness of strip samples after repetitive corrugation and straightening increases over two times when compared to the samples after annealing (Fig. 14). In the samples subjected to RCS process increase of hardness with increase of the number of cycles is registered, however in the samples after maximum number of cycles slight decrease of hardness was observed in comparison to the samples subjected to 2/3 of the critical number of cycles, which can show presence of some critical value of deformation above which hardness increase is not observed, probably due to processes of dynamic recovery which decreases density of dislocations in the material. Hardness of strip samples after RCS process and the next annealing decrease to value of samples in the initial state.

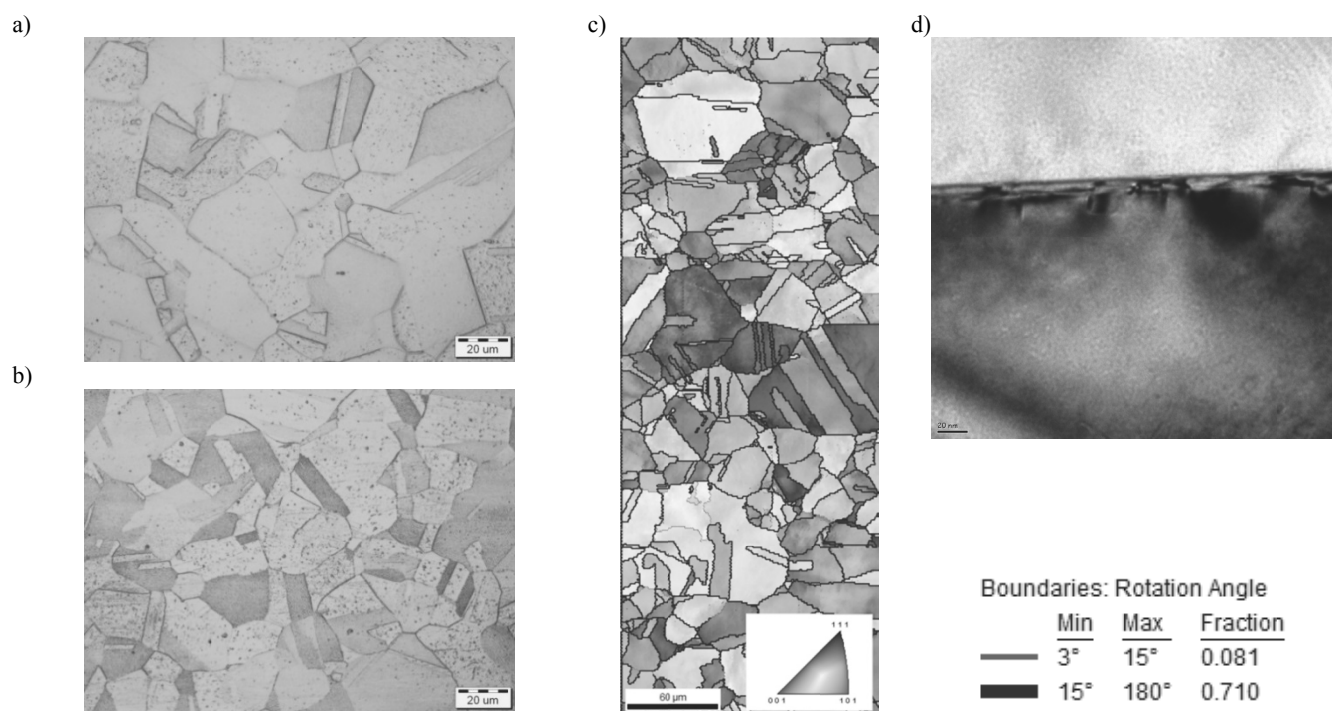


Fig. 1. Microstructure of Cu after annealing in temperature of 550°C/1h, a) light microscopy- longitudinal section, b) light microscopy - transverse section, c) orientation distribution of grains with marked boundaries wide-angle (thick lines) and narrow-angle (thin lines), d) TEM

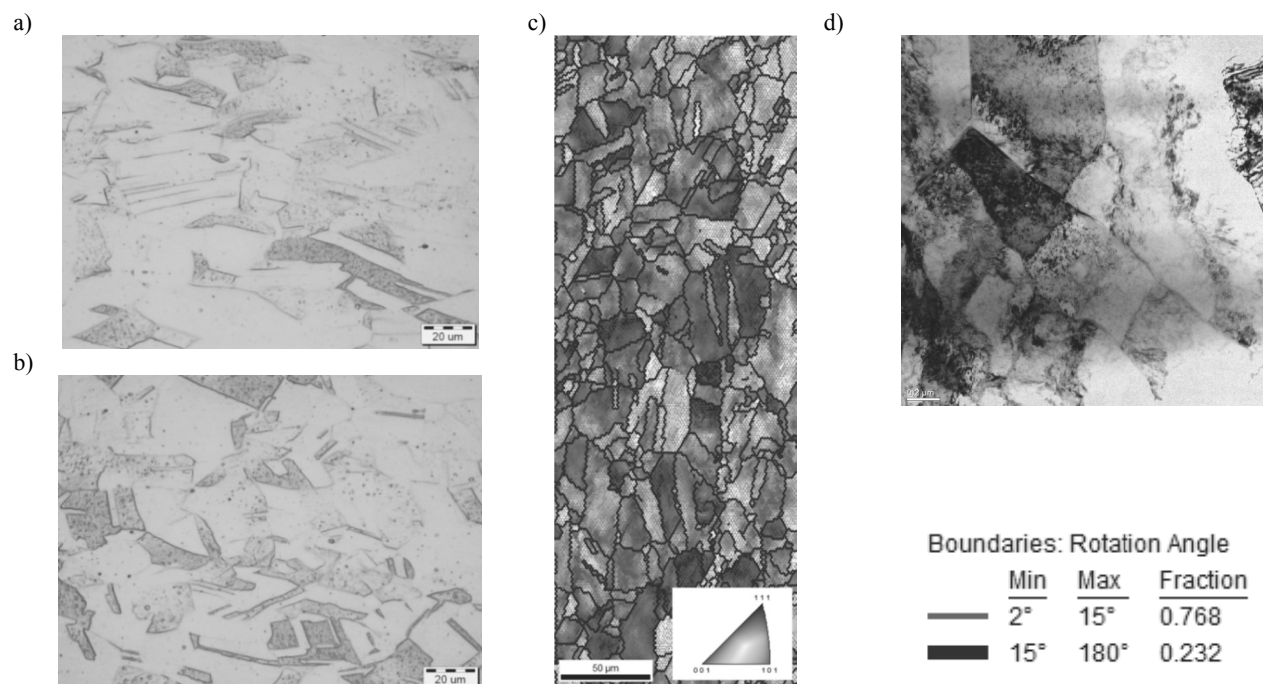


Fig. 2. Microstructure of Cu strip deformed after 42 cycles of RCS process, a) light microscopy- longitudinal section, b) light microscopy - transverse section, c) orientation distribution of grains with marked boundaries wide-angle (thick lines) and narrow-angle (thin lines), d) TEM



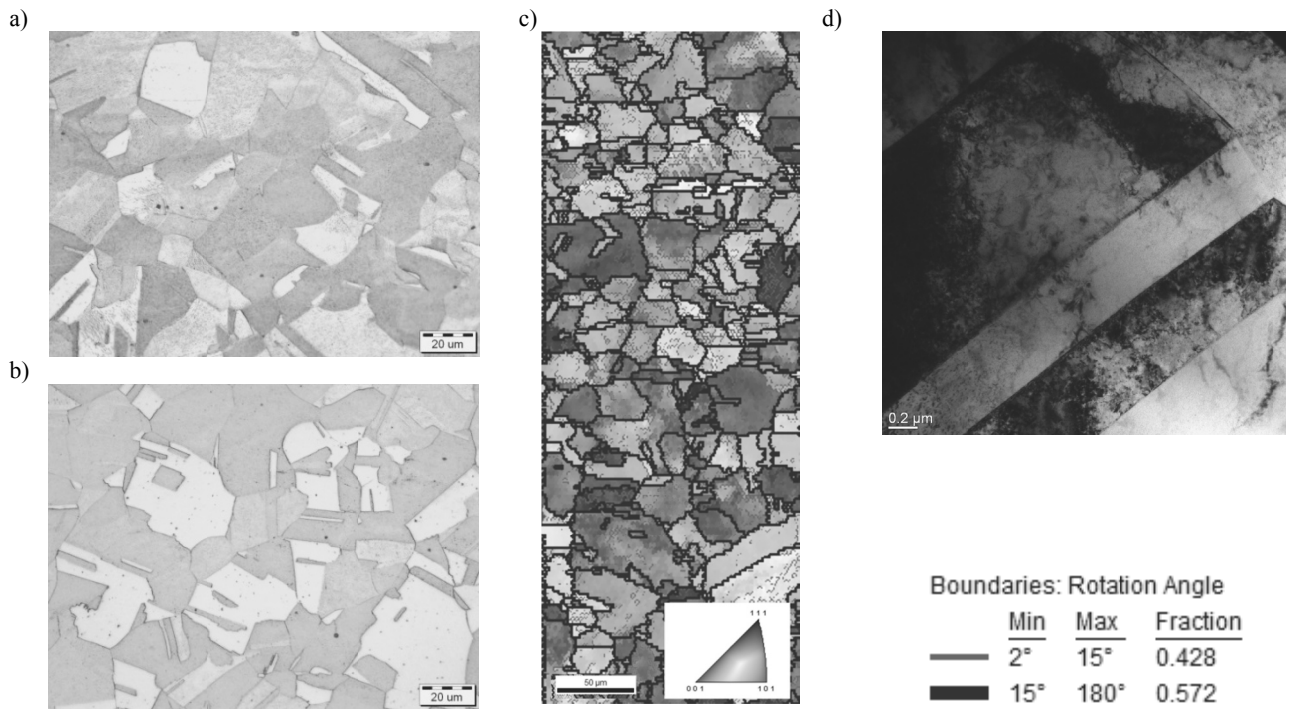


Fig. 3. Microstructure of Cu strip deformed after 42 cycles of RCS process and after annealing in temperature of 550°C/1h, a) light microscopy- longitudinal section, b) light microscopy - transverse section, c) orientation distribution of grains with marked boundaries wide-angle (thick lines) and narrow-angle (thin lines), d), TEM

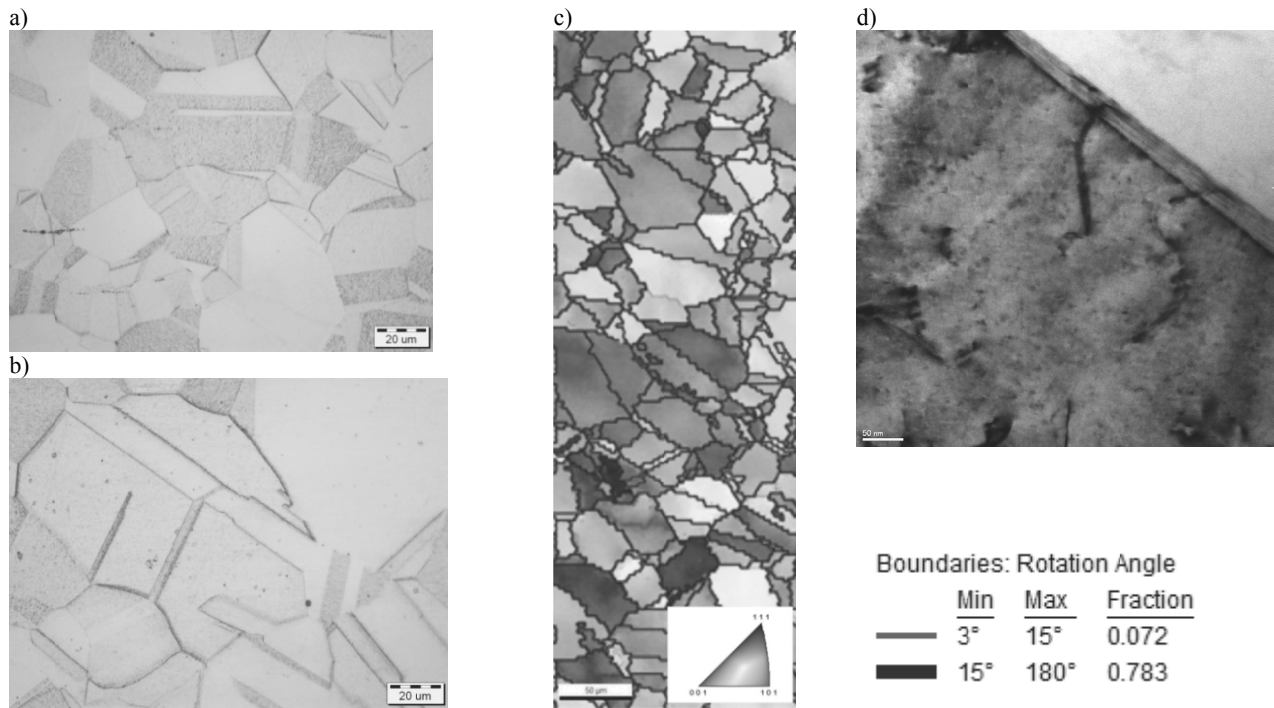


Fig. 4. Microstructure of CuZn36 after annealing in temperature of 550°C/1h, a) light microscopy- longitudinal section, b) light microscopy - transverse section, c) orientation distribution of grains with marked boundaries wide-angle (thick lines) and narrow-angle (thin lines), d) TEM

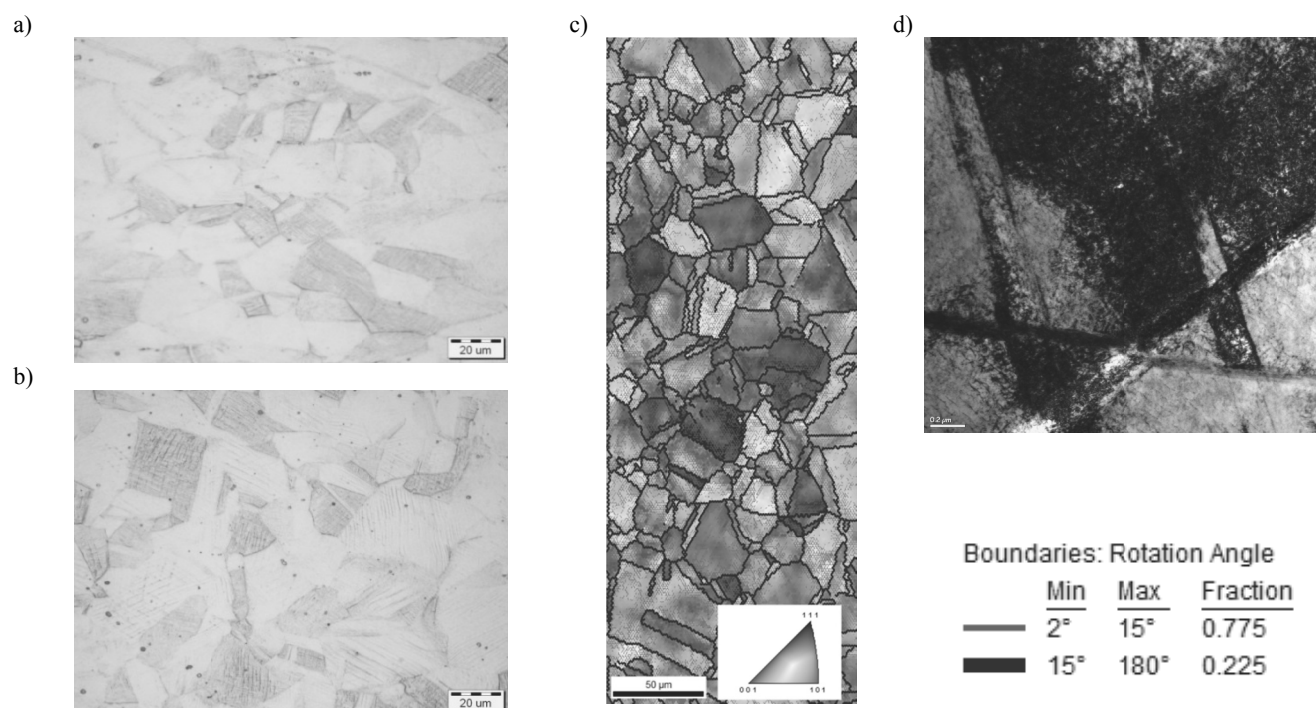


Fig. 5. Microstructure of CuZn36 strip deformed after 36 cycles of RCS process, a) light microscopy- longitudinal section, b) light microscopy - transverse section, c) orientation distribution of grains with marked boundaries wide-angle (thick lines) and narrow-angle (thin lines), d) TEM

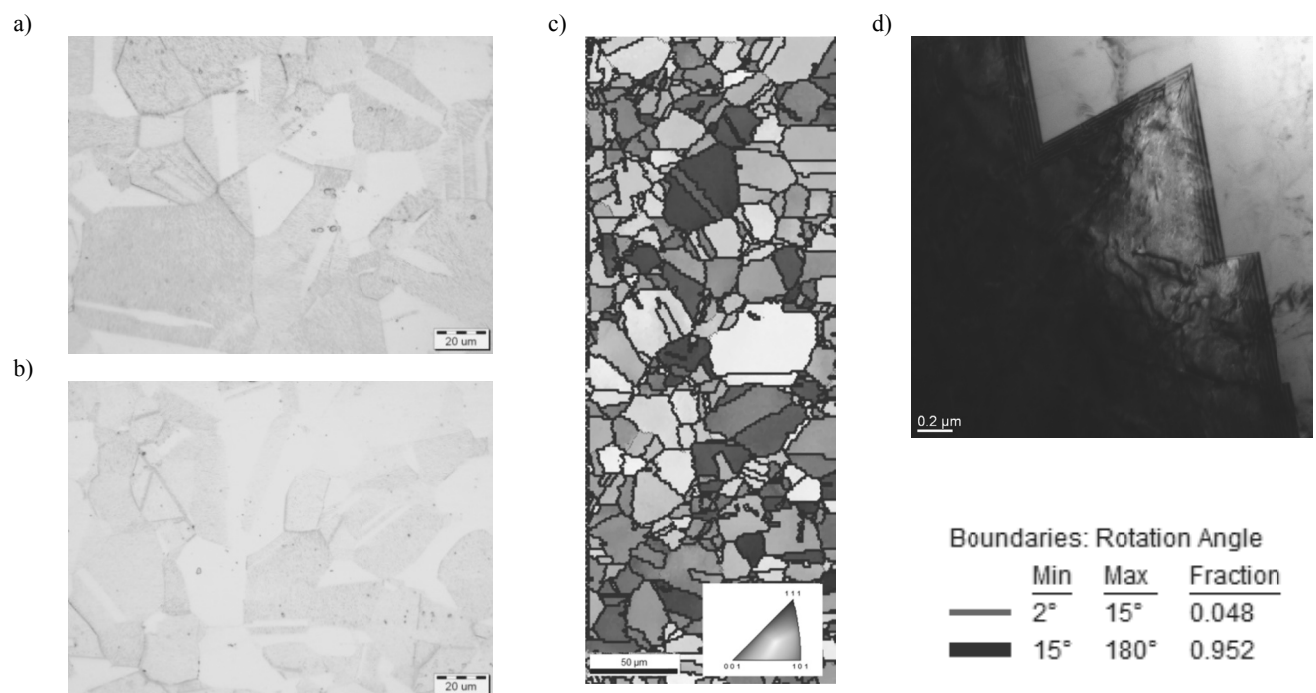


Fig. 6. Microstructure of CuZn36 strip deformed after 36 cycles of RCS process and after annealing in temperature of 550°C/1h, a) light microscopy- longitudinal section, b) light microscopy - transverse section, c) orientation distribution of grains with marked boundaries wide-angle (thick lines) and narrow-angle (thin lines), d) TEM



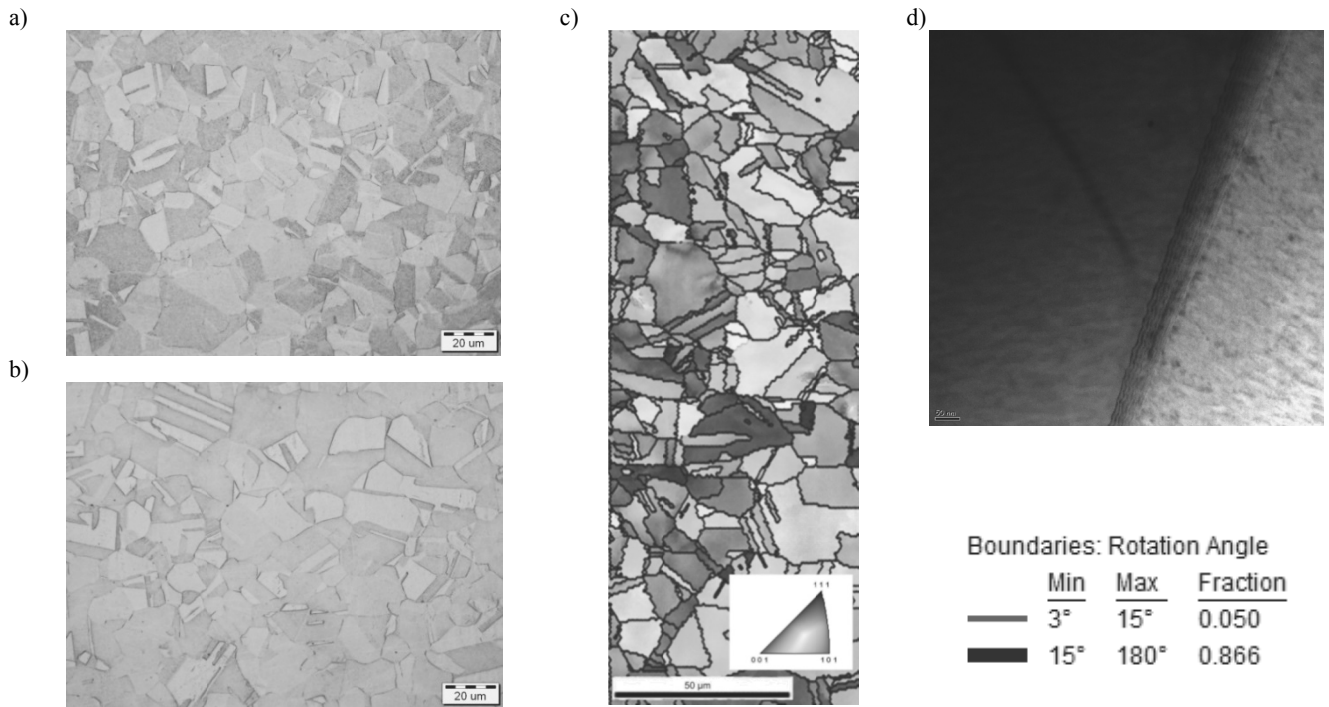


Fig. 7. Microstructure of CuSn6 after annealing in temperature of 550°C/1h, a) light microscopy- longitudinal section, b) light microscopy - transverse section, c) orientation distribution of grains with marked boundaries wide-angle (thick lines) and narrow-angle (thin lines), d) TEM

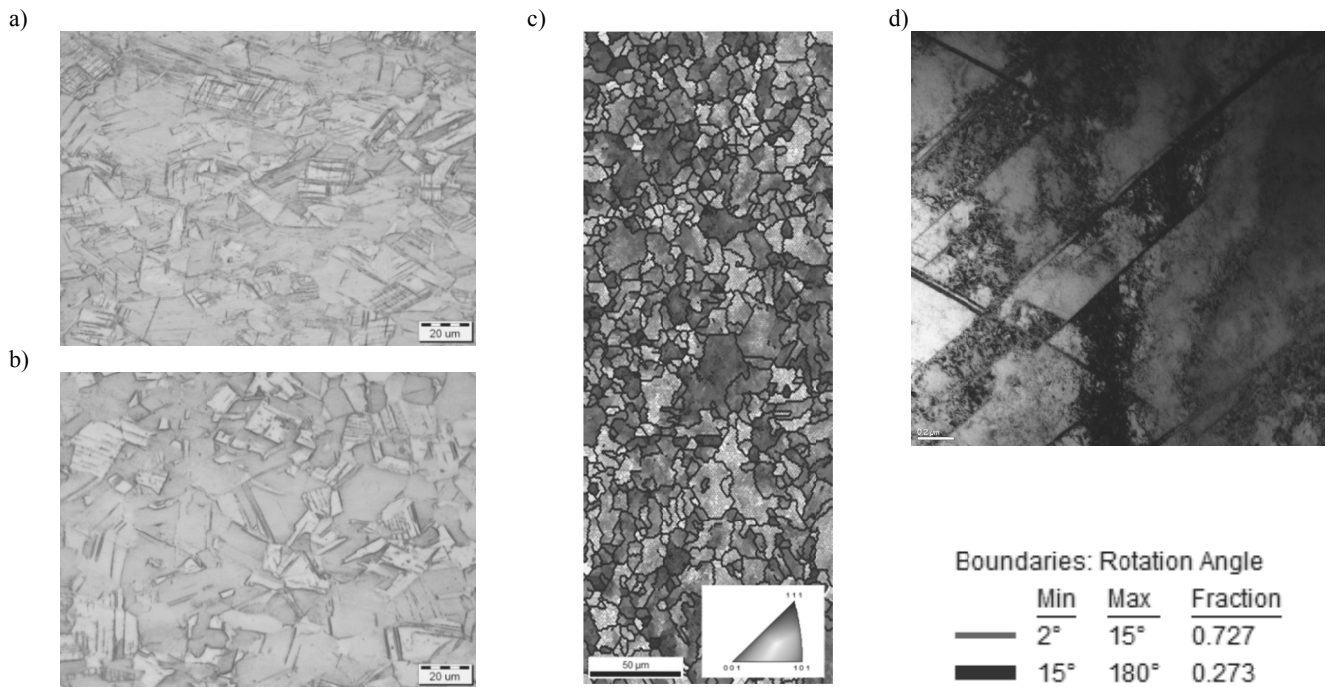


Fig. 8. Microstructure of CuSn6 strip deformed after 52 cycles of RCS process, a) light microscopy- longitudinal section, b) light microscopy - transverse section, c) orientation distribution of grains with marked boundaries wide-angle (thick lines) and narrow-angle (thin lines), d) TEM

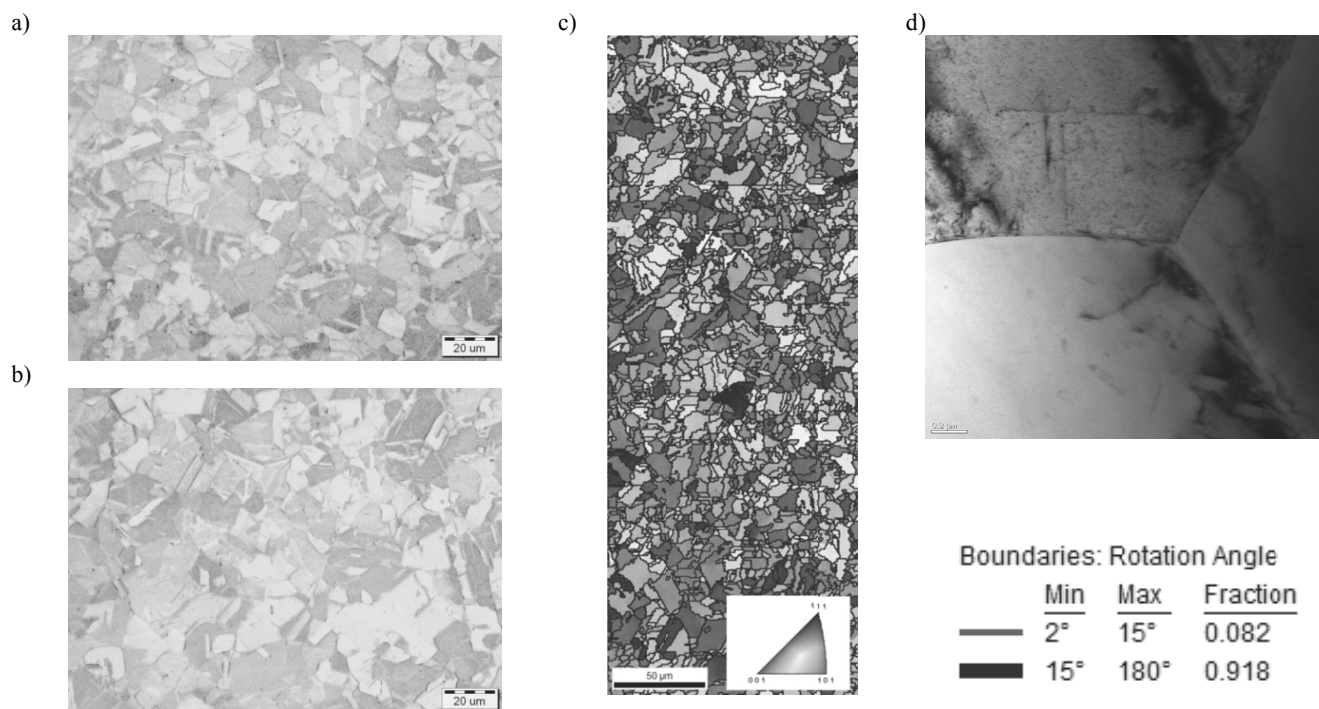


Fig. 9. Microstructure of CuSn6 strip deformed after 52 cycles of RCS process after annealing in temperature of 550°C/1h, a) light microscopy- longitudinal section, b) light microscopy - transverse section, c) orientation distribution of grains with marked boundaries wide-angle (thick lines) and narrow-angle (thin lines), d) TEM

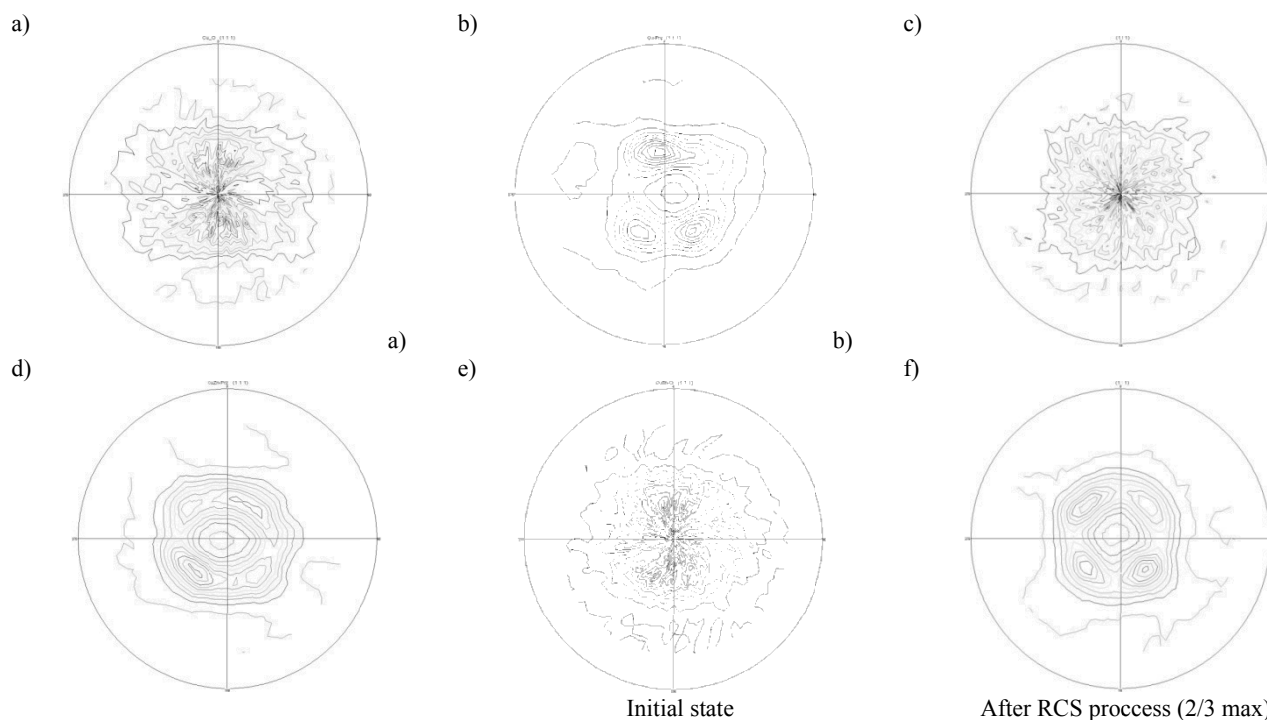


Fig. 10. Texture of strip samples Cu (a, b), CuZn36 (c, d) and CuSn6 (e, f), in initial state and after repetitive corrugation and straightening, respectively



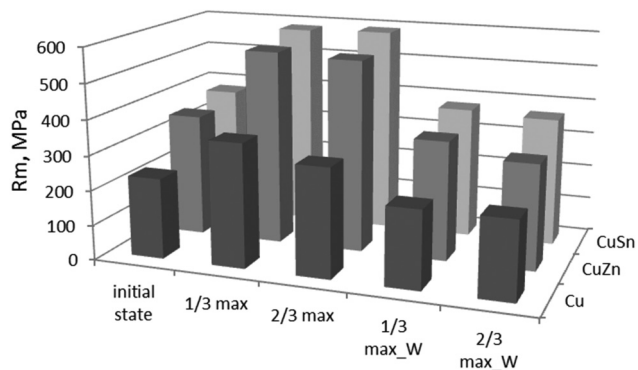


Fig. 11. Tensile strength of Cu, CuZn36, CuSn6 strips after annealing (initial state), after deformation by RCS method (1/3 max, 2/3 max), after deformation by RCS method and next annealing (1/3max\_W, 2/3max\_W)

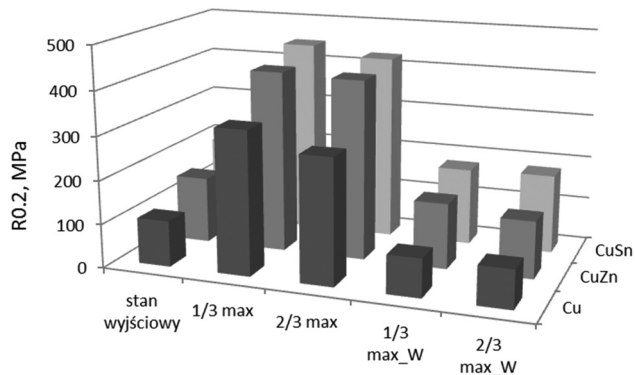


Fig. 12. 0.2 yield strength of Cu, CuZn36, CuSn6 strips after annealing, after deformation by RCS method (1/3 max, 2/3 max), after deformation by RCS method and next annealing (1/3max\_W, 2/3max\_W)

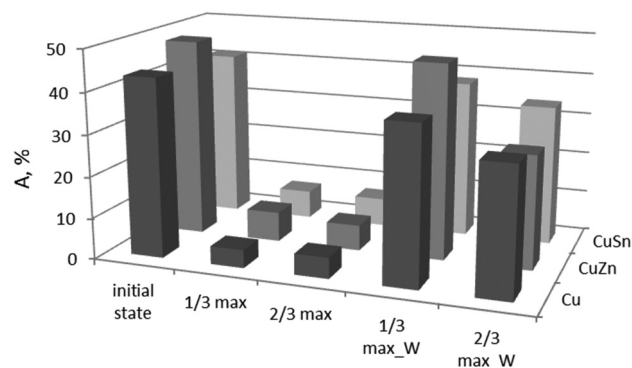


Fig. 13. Elongation of Cu, CuZn36, CuSn6 strips after annealing and after deformation by RCS method (1/3 max, 2/3 max), after deformation by RCS method and next annealing (1/3max\_W, 2/3max\_W)

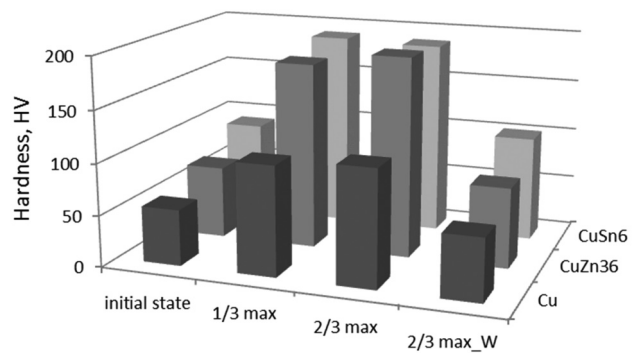


Fig. 14. Hardness of Cu, CuZn36 and CuSn6 strips in the initial state, after deformation by RCS method (1/3 max, 2/3 max), after deformation by RCS method and next annealing (2/3max\_W)

Electrical conductivity after RCS process of copper samples is about 57 MS/m, of CuZn36 samples about 15 MS/m, while of CuSn6 samples it is about 9 MS/m, which is 93-96% of electrical conductivity of samples in annealed state (Fig. 15).

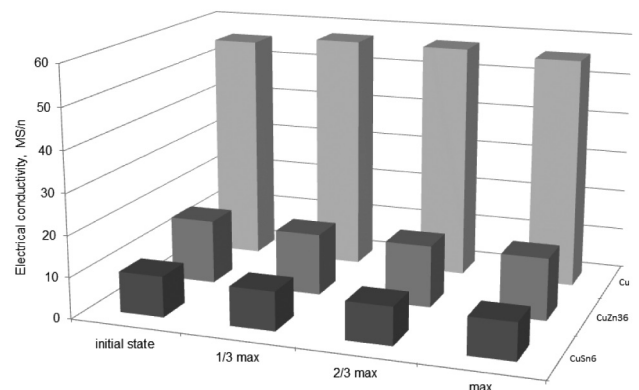


Fig. 15. Electrical conductivity of Cu, CuZn36 and CuSn6 strips in the initial state and after deformation by RCS method

### 3.2. Industrial tests

Fig. 16 shows the microstructure of the CuSn6 strip samples before testing, while in Fig. 17 after four RCS passes. The microstructure of the samples after corrugation and straightening is characterized by pronounced effects of cold deformation.

Mechanical properties of CuSn6 strip were tension tested in three directions: along the rolling direction 0°, perpendicular to the rolling direction 90° and 45° to the rolling direction. There was a downward trend in tensile strength with increasing number of cycles of RCS (Fig. 18). The highest values were observed in the specimens cut perpendicular to the rolling direction. On samples cut in the rolling direction - 0° and 45° to the rolling direction similar values of tensile strength were observed. The value of the yield strength for the rolling direction 0° were in the

range from 458 MPa to 370 MPa, perpendicular to the rolling direction 90° were from 453 MPa to 435 MPa. However, 45° to the rolling direction were in the range 450-441 MPa. For samples taken perpendicular to the rolling direction 90° decrease and then increase in yield strength were observed while increasing of cycle numbers RCS process (Fig 19).

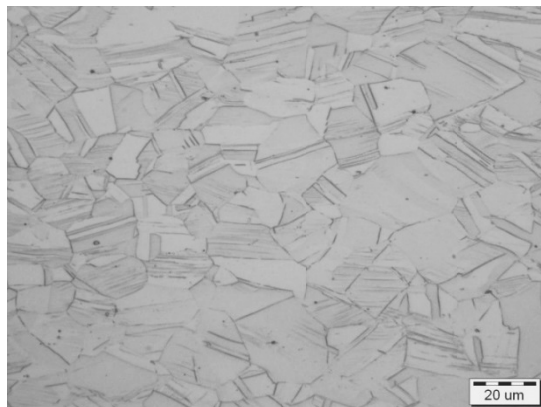


Fig. 16. Microstructure of CuSn6 strip deformed before RCS process, perpendicular to the rolling direction



Fig. 17. Microstructure of CuSn6 strip deformed after 4 passes of RCS process, perpendicular to the rolling direction

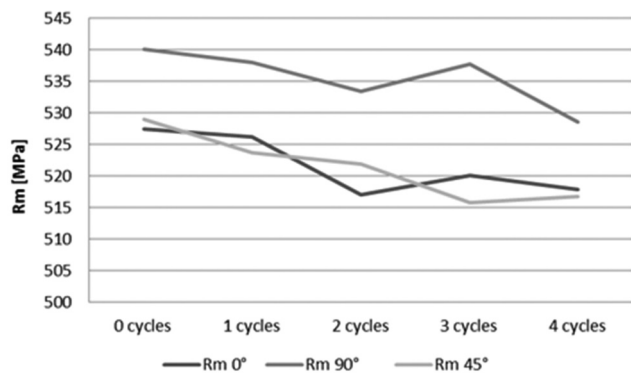


Fig. 18. Tensile strength of CuSn6 strip during RCS process

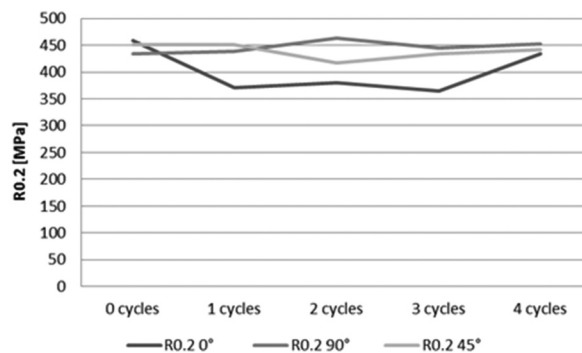


Fig. 19. Yield strength of CuSn6 strip during RCS process

Elongation of CuSn6 samples during RCS process maintained at the same level. For 0° sample A20 was about 22, for 90° sample A20 = 15, and for 45° sample A20 = 18.

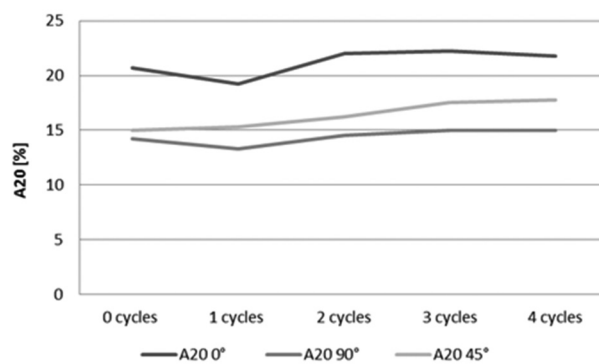


Fig. 20. Elongation of CuSn6 strip during RCS process

With increasing of number of passes the tape roll alignment hardness values were observed for samples tested along and perpendicular to the rolling direction.

Hardness leveling in 0° 90° directions were observed during RCS process (Fig. 21). The initial difference of hardness in 0° 90° directions was about 28HV. However, after four RCS cycles the difference in hardness was about 7 HV only.

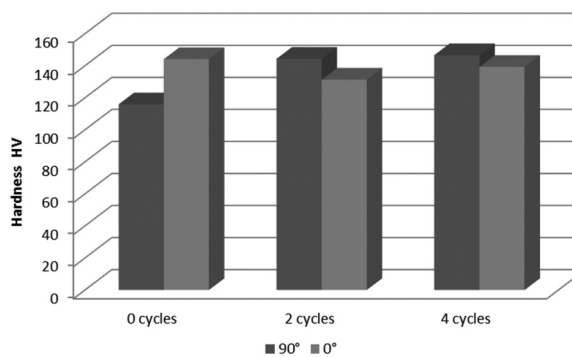


Fig. 21. Hardness of CuSn6 strip during RCS process

## 4. Conclusions

The RCS process is an efficient method for microstructure refinement. The refinement results from formation of grains/subgrains of misorientation angle up to  $8^\circ$  mostly. Mechanism of subgrain formation in the process of complex deformation results from shearing of initiated slip systems within individual grains. Grains of high-angle boundaries are formed mainly in the areas of crisscrossing shearing bands.

Mechanical properties ( $R_m$ ,  $R_{0.2}$ , HV) of strips after RCS process are significantly higher than in the strips after annealing and also after RCS process and next annealing.

No significant changes of electrical conductivity were observed with the change of sample deformation. It is possible to design ultrafine alloys of high strength by adjustment of stacking fault energy SFE.

The RCS allows to control the mechanical properties of copper alloys in wide range and the cold deformation RCS effects are reversible by annealing operations.

## Acknowledgements

The study was conducted within the scope of Development Project POIG.01.01.02-00-015/09 "Advanced materials and technologies for their production".

The authors wish to thank the Menagement of WM Dziedzice rolling plant for enabling of industrial tests.

The authors wish to thank dr Mariusz Staszewski for carrying out the XRD examinations.



## References

- [1] J. Huang, Y. Zhu, H. Jiang, T. Lowe, Microstructures and dislocation configurations in nanostructured Cu processed by repetitive corrugation and straightening, *Acta Materialia* 49 (2001) 1497-1505.
- [2] Y. Zhu, J. Huang, H. Jiang, T. Lowe, Processing of bulk nanostructured copper by repetitive corrugation and straightening, *Proceeding of 2<sup>nd</sup> Global Symposium on Innovations in Materials Processing and Manufacturing - Sheet Materials*, TMS Annual Meeting, New Orleans, 2001.
- [3] R. Asaro, P. Krysl, D. Benson, Deformation mechanism and manufacturing of nanostructured materials processed by severe plastic deformation (SPD) NSF Nanoscale, *Proceedings of the Science and Engineering Grantees Conference*, 2003, 16-18.
- [4] J.Y. Huang, X.Z. Liao, Y.T. Zhu, F. Zhou, E.J. Lavernia, Grain boundary structure of nanocrystalline Cu processed by cryomilling, *Philosophical Magazine* 83/12 (2003) 1407-1419.
- [5] J. Huang, Y.T. Zhu, D.J. Alexander, X. Liao, T.C. Lowe, R.J. Asaro, Development of repetitive corrugation and straightening, *Materials Science and Engineering A* 371 (2004) 35-39.
- [6] F.A. Mohamed, Y. Xun, Correlations between the minimum grain size produced by milling and material parameters, *Materials Science and Engineering A* 354 (2003) 133-139.
- [7] H.-J. Fecht, Nanostructure formation by mechanical attrition, *Nano Structured Materials* 6 (1995) 33-42.
- [8] A. Mishra, V. Richard, F. Gregori, R.J. Asaro, M.A. Meyers, Microstructural evolution in copper processed by severe plastic deformation, *Materials Science and Engineering A* 410-411 (2005) 290-298.
- [9] M.A. Meyers, V.F. Nesterenko, J.C. LaSalvia, Q. Xue, Shear localization in dynamic deformation of materials: microstructural evolution and self-organization, *Materials Science and Engineering A* 317 (2001) 204-225.
- [10] Y.H. Zhao, Y.T. Zhu, X.Z. Liao, Z. Horita, T.G. Langdon, Influence of stacking fault energy on minimum grain size achieved in severe plastic deformation, *Materials Science and Engineering A* 463 (2007) 22-26.
- [11] Y.H. Zhao, X.Z. Liao, Z. Horita, T.G. Langdon, Y.T. Zhu, Determining the optimal stacking fault energy for achieving high ductility in ultrafine-grained Cu-Zn alloys, *Materials Science and Engineering A* 493/1-2 (2008) 123-129.
- [12] K.S. Kumar, H. Van Swygenhoven, S. Suresh, Mechanical behavior of nanocrystalline metals and alloys, *Acta Materialia* 51 (2003) 5743-5774.
- [13] J. Stobrawa, Z. Rdzawski, W. Głuchowski, W. Malec, Microstructure refining of CuNi2Si1 alloy using RCS method, conference materials, *Proceedings of the XXXVII School of Materials Science and Engineering* Cracow-Krynica, 2009, 139-143
- [14] J. Stobrawa, Z. Rdzawski, W. Głuchowski, W. Malec, Ultrafine grained strip of CuCr0,6 alloy prepared by CRCS metod, *Journal of Achievements in Materials and Manufacturing Engineering* 33/2 (2009) 166-172.
- [15] J. Stobrawa, Z. Rdzawski, W. Głuchowski, W. Malec, Microstructure and properties of CuNi2Si1 alloy processed by continuous RCS method, *Journal of Achievements in Materials and Manufacturing Engineering* 37/2 (2009) 466-479.
- [16] J. Stobrawa, Z. Rdzawski, W. Głuchowski, W. Malec, Microstructure evolution in CRCS processed strips of CuCr0.6 alloy, *Journal of Achievements in Materials and Manufacturing Engineering* 38/2 (2010) 195-202.
- [17] J. Stobrawa, Z. Rdzawski, W. Głuchowski, W. Malec, Ultrafine grained strips of precipitation hardened copper alloys, *Archives of Metallurgy and Materials* 56 (2011) 171-179.
- [18] J. Stobrawa, J. Domagała-Dubiel, W. Głuchowski, J. Sobota, Microstructure and properties of CuSn6 strips processed by continuous RCS method, *Proceedings of the XL School of Materials Engineering*, Cracow, 2012, 416-420.
- [19] S.Ch. Yoon, U. Krishnaiah, Chakkingal, H.S. Kim, Severe plastic deformation and strain localization in groove pressing, *Computational Materials Science* 43 (2008) 641-645.
- [20] S.N. Dey, P. Chatterjee, S.P. Sen Gupta, Deformation stacking fault propability and dislocation microstructure of cold worked Cu-Sn-5Zn alloys by X-ray diffraction line profile analysis, *Journal of Applied Physics* 100/7 (2006).